



# Effect of Sr substitution on electrical transport and thermoelectric properties of $Y_{1-x}Sr_xCoO_3$ ( $0 \leq x \leq 0.2$ ) prepared by sol–gel process

Yi Liu<sup>a,b,\*</sup>, Haijin Li<sup>a,b</sup>, Yong Li<sup>a,b</sup>, Wenbin Sun<sup>a</sup>

<sup>a</sup>School of Mathematics and Physics, Anhui University of Technology, 243032 Maanshan, PR China

<sup>b</sup>Institute of Optoelectronic Information Materials and Technology, Anhui University of Technology, 243032 Maanshan, PR China

Received 24 January 2013; received in revised form 22 March 2013; accepted 30 March 2013

Available online 8 April 2013

## Abstract

The effect of Sr substitution on electrical transport and thermoelectric properties of  $Y_{1-x}Sr_xCoO_3$  ( $0 \leq x \leq 0.2$ ) has been investigated in the temperature range from 20 to 780 K. The  $Y_{1-x}Sr_xCoO_3$  samples with different Sr concentrations have been synthesized by using the sol–gel process. The results show that dc electrical resistivity of  $Y_{1-x}Sr_xCoO_3$  decreases remarkably with increasing Sr content  $x$ , which can be attributed to the reduction in lattice distortion. The Seebeck coefficients  $S$  of  $Y_{1-x}Sr_xCoO_3$  are all positive, indicating predominant hole-type charge carriers, and they decrease monotonously with increasing Sr content of substitution. Moreover, experiments show that the power factor changes non-monotonously with Sr substitution with a maximum value of  $2.69 \times 10^{-5}$  W/m K<sup>2</sup> at 650 K for the sample  $x=0.05$ , which is about five times greater than that for  $x=0$ , indicating that appropriate Sr substitution can effectively improve thermoelectric properties of  $Y_{1-x}Sr_xCoO_3$ .

© 2013 Elsevier Ltd and Techna Group S.r.l. All rights reserved.

**Keywords:** A. Sol–gel processes; C. Electrical properties; D. Transition metal oxides

## 1. Introduction

In recent decades thermoelectric materials have renewedly attracted extensive attention due to their great application in clean power generation using the Seebeck effect and refrigeration by the Peltier effect amidst polluted environment and energy crisis. Thermoelectric performance for thermoelectric materials is characterized in terms of a dimensionless figure of merit  $ZT = S^2T/(\rho\kappa)$ , where  $S$  is the Seebeck coefficient or thermopower,  $\rho$  is the electrical resistivity,  $\kappa$  is the total thermal conductivity,  $T$  is the absolute temperature, and the power factor  $P$  is given by the expression  $P = S^2/\rho$  [1]. Therefore, a thermoelectric material with good thermoelectric performance should have large thermopower with small electrical resistivity and thermal conductivity.

Recently, metal oxides have been considered as good candidates as thermoelectric materials due to, compared with the traditional materials, such as  $Bi_2Te_3$ ,  $CoSb_3$ ,  $Si_{1-x}Ge_x$  etc,

their easy fabrication, low cost, and high thermal and chemical stability at high temperature in air. In 1997, Terasaki et al. [2] reported that the single crystal  $NaCo_2O_4$  exhibited a good thermoelectric performance with thermopower  $S \sim 100$   $\mu$ V/K and resistivity  $\rho \sim 200$   $\mu\Omega$  cm at 300 K. One after the other, in 2004, Androulakis and Pantelis Migiakis [3] found a very respectable room-temperature oxide thermoelectric material  $La_{0.95}Sr_{0.05}CoO_3$  with the value of figure of merit 0.18. In last several years, our group [4–8], in addition to other authors [9,10], has also considered  $YCoO_3$  (a distorted perovskite structure [11,12] with orthorhombic symmetry, space group  $Pbnm$   $Z=4$ , where six oxygen atoms surround each cobalt ion) as a thermoelectric material and investigated it, because of its large thermopower  $S \sim 1039$   $\mu$ V/K [5] and small thermal conductivity  $\kappa \sim 5.39$  W/m K [5] in the vicinity of room temperature, which are two preconditions for having good thermoelectric performance (i.e. large  $ZT$  value). This is already fulfilled for the  $YCoO_3$  series. However, it has large electrical resistivity (such as  $\rho \sim 6.9$   $\Omega$  m at 300 K [4]), which is a disadvantage as a thermoelectric material. Our group [4] and Hejtmánek et al. [9,10] have succeeded in decreasing its electrical resistivity by substituting Ca for Y, and we estimated the thermoelectric performance ( $ZT \sim 0.019$  at 660 K). Our

\*Corresponding author at: Anhui University of Technology, School of Mathematics and Physics, Ma Xiang Road, Maanshan 243032, China. Tel.: +86 555 2315212.

E-mail address: [yliu6@ahut.edu.cn](mailto:yliu6@ahut.edu.cn) (Y. Liu).

investigation and the suggestions given by the researchers for similar system  $R_{1-x}Ca_xCoO_3$  ( $R=Ho, Dy, Gd, Sm, Nd, \text{ and } Pr$ ) [13–15] indicated that the decrease of lattice distortion degree of  $YCoO_3$  by the substitution of large ion radius  $Ca^{2+}$  (0.99 Å) for  $Y^{3+}$  (0.89 Å) or larger rare-earth ion for small rare-earth ion might be advantageous for decreasing its electrical resistivity and improving its thermopower. Thus, can the substitution of much larger  $Sr^{2+}$  (1.12 Å) ( $Sr^{2+} > Ca^{2+}$  in ion radius) for  $Y$  in  $YCoO_3$  can enhance more effectively its thermoelectric performance? Moreover, as far as we know, the electrical transport and thermoelectric properties of the substitution of  $Sr$  for  $Y$  in  $YCoO_3$  have been scarcely investigated except for the investigation of  $Y_{1-x}Sr_xCoO_3$  film as a gas sensor by Michel et al. [16]. At present, we report the effect of substitution of  $Sr$  for  $Y$  in  $YCoO_3$  on electrical transport and thermoelectric properties in the temperature range from 20 to 780 K.

## 2. Experimental details

Strontium doped yttrium oxides were prepared from stoichiometric amounts of strontium, cobalt and yttrium nitrates.  $0.02x$  ( $x=0, 0.01, 0.05, 0.15, \text{ and } 0.20$ ) mol of  $Sr(NO_3)_2$  (99.5%),  $0.02(1-x)$  mol of  $Co(NO_3)_2 \cdot 6H_2O$  (99.0%), and  $0.02$  mol of  $Y(NO_3)_3 \cdot 6H_2O$  (99.0%) were dissolved in 20 ml of an aqueous solution of 0.02 mol citric acid (99.5%) using de-ionized water. The solutions were continuously stirred for about 1 h, resulting in a

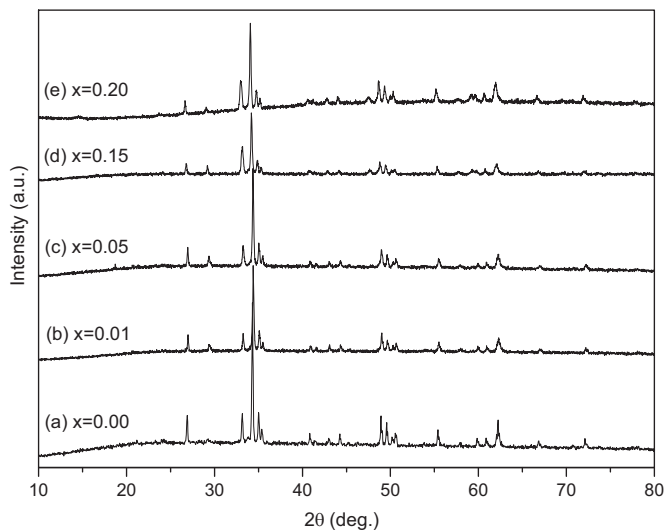


Fig. 1. XRD patterns ( $CuK_{\alpha}$  irradiation) for  $Y_{1-x}Sr_xCoO_3$  ( $x=0, 0.01, 0.05, 0.15, 0.2$ ).

Table 1

The room temperature lattice parameters  $a$ ,  $b$  and  $c$ , and unit cell volume  $V$ .

$x$	$a$ (Å)	$b$ (Å)	$c$ (Å)	$V$ (Å <sup>3</sup> )
0.00	$5.1393(\pm 2.6 \times 10^{-4})$	$5.4197(\pm 2.7 \times 10^{-4})$	$7.4588(\pm 3.7 \times 10^{-4})$	$207.75(\pm 0.01)$
0.01	$5.1406(\pm 2.6 \times 10^{-4})$	$5.4182(\pm 2.7 \times 10^{-4})$	$7.4591(\pm 3.7 \times 10^{-4})$	$207.76(\pm 0.01)$
0.05	$5.1437(\pm 2.6 \times 10^{-4})$	$5.4181(\pm 2.7 \times 10^{-4})$	$7.4611(\pm 3.7 \times 10^{-4})$	$207.93(\pm 0.01)$
0.15	$5.1445(\pm 2.6 \times 10^{-4})$	$5.4153(\pm 2.7 \times 10^{-4})$	$7.4602(\pm 3.7 \times 10^{-4})$	$207.83(\pm 0.01)$
0.20	$5.1443(\pm 2.6 \times 10^{-4})$	$5.4204(\pm 2.7 \times 10^{-4})$	$7.4605(\pm 3.7 \times 10^{-4})$	$208.03(\pm 0.01)$

homogenization of  $Sr^{2+}$ ,  $Co^{2+}$  and  $Y^{3+}$  cations in the mixture solution. Subsequently, the mixtures were slowly heated to 90 °C, and at this temperature they were dried for 12 h forming a brown powder from the mixtures. The brown powders were calcined in air at atmospheric pressure in a muffle furnace at 300 °C for 2 h, forming black powder samples so as to remove organic compounds. Then, these powder samples were ground and subsequently compressed into pellets 13 cm in diameter. Finally, bulk samples were obtained by sintering the green pellets in air in a tube furnace at 900 °C for 120 h, subsequently followed by spontaneous cooling slowly down to room temperature in the furnace.

Phase structures and lattice constant for the obtained compounds were characterized by using XRD (Philips-XPERT PRO diffractometer) with  $Cu K_{\alpha}$  irradiation ( $\lambda=0.154056$  nm) at room temperature. The accurate lattice parameters were determined from the  $d$ -value of the XRD peaks using a standard least-square refinement method with a Si standard for calibration. To measure their electrical resistivity, bar-shaped specimens of the size ( $\sim$ )12 mm  $\times$  ( $\sim$ )2 mm  $\times$  ( $\sim$ )1.0 mm were cut from the bulk samples. The electrical resistivity and Seebeck coefficient were measured on a computer-assisted device. DC electrical resistivity was measured in vacuum by a conventional standard four-probe method at the temperatures from 20 to 720 K. Seebeck coefficient was also measured in vacuum in a temperature range from 300 to 780 K. The power factor was calculated from the above-measured  $S$  and  $\rho$  parameters.

## 3. Results and discussion

### 3.1. Phase determination, change of lattice parameters and lattice distortion degree for $Y_{1-x}Sr_xCoO_3$

Fig. 1 presents the XRD patterns of  $Y_{1-x}Sr_xCoO_3$  ( $x=0, 0.01, 0.05, 0.15, \text{ and } 0.20$ ) with different strontium contents at room temperature. The main diffraction peaks of XRD patterns for synthesized  $YCoO_3$  are very consistent with what is indexed based on the standard JCPDS card (No. 88-0425) of  $YCoO_3$ . We can observe from Fig. 1 that the main peaks of the doped samples  $Y_{1-x}Sr_xCoO_3$  ( $x \neq 0$ ) are in agreement with that of the synthesized sample  $YCoO_3$ , indicating that the substitution of  $Sr$  for  $Y$  in  $YCoO_3$  has taken place and the substituted compounds have formed.

To check the deformation degree of the  $YCoO_3$  lattice after  $Sr$  substitution, accurate lattice constants  $a$ ,  $b$  and  $c$  are measured from the XRD data, as listed in Table 1, whose values are consistent with other literature data [12]. One can

note that the lattice parameters of  $Y_{1-x}Sr_xCoO_3$  change as the substituted Sr content increases. The lattice parameter  $a$ , firstly, increases rapidly with the increasing Sr content (such as 5.1393 Å for  $x=0$  to 5.1406 Å for  $x=0.01$  and 5.1437 Å for  $x=0.05$ ); then the lattice constant  $a$  has scarcely obvious change (for instance, 5.1445 Å for  $x=0.15$  and 5.1443 Å for  $x=0.20$ ) within the experimental error. Moreover, the lattice constant  $c$  also firstly increases from 7.4588 Å for  $x=0$  to 7.4591 Å for  $x=0.01$  and subsequently to 7.4611 Å for  $x=0.05$ ; then decreases to 7.4602 Å for  $x=0.15$  and 7.4605 Å for  $x=0.2$ . The results, on the other hand, imply that the substitution of Sr for Y in  $YCoO_3$  lattice has indeed taken place, and indicate that the Sr substitution leads to the change of distortion degree of  $YCoO_3$ , which is also reflected in the change of volume of unit cell (calculated from the lattice constants  $a$ ,  $b$  and  $c$ ) of  $Y_{1-x}Sr_xCoO_3$ , such as 207.75 Å<sup>3</sup> for  $x=0$  and 208.03 Å<sup>3</sup> for  $x=0.2$ , as listed in Table 1. From Table 1 we can note that there is no monotonic dependence between composition and unit cell parameters, which can be due to the production of  $[Co_{Co}]$  species (see the following discussion). We also obtain from the calculation of lattice parameters  $a$ – $c$  the relation  $a < c/\sqrt{2} < b$  for all the samples  $Y_{1-x}Sr_xCoO_3$ , indicating that lattice structure of these samples belongs to so-called typical O-type structure and the distortion of lattice in  $YCoO_3$  is relatively small after Sr substitution [17]. The main source of small distortion is the buckling of the octahedral  $CoO_6$  network, which also is suggested by another author [17]. We also can adopt the Goldschmidt tolerance factor  $t$  to qualitatively estimate the structural distortion degree in perovskites with the general formula  $RCO_3$ . The following is the expression equation [18]:

$$t = \frac{r_R + r_O}{\sqrt{2}(r_{Co} + r_O)} \quad (1)$$

where  $r_R$ ,  $r_{Co}$  and  $r_O$  represent the average ionic radii of the respective cations R, Co and anion oxygen, respectively. Assume that the average ionic radius of Co and O is invariable at room temperature. Therefore, since the ion radius of  $Sr^{2+}$  (1.12 Å) is bigger than  $Y^{3+}$  (0.89 Å), the tolerance factor  $t$  increases with increasing doped Sr content  $x$ , leading to the decrease in lattice distortion as  $x$  increases [19]. The decrease of distortion may be caused by the partial substitution of Sr for Y, and this also would affect the transport properties of  $Y_{1-x}Sr_xCoO_3$  (see following sections), as suggested by Liu et al. [5], Mehta et al. [11], Knížek et al. [12] and Ji-Woong Moon et al. [13].

### 3.2. Resistivity and its temperature dependences for $Y_{1-x}Sr_xCoO_3$

Fig. 2 plots the dc electrical resistivity  $\rho$  as a function of temperature  $T$  for  $Y_{1-x}Sr_xCoO_3$  ( $x=0, 0.01, 0.05, 0.15$ , and 0.20) in the temperature range from 20 to 720 K. We note that at low temperatures  $YCoO_3$  is a good insulator ( $6.54 \times 10^3 \Omega m$  at  $\sim 190$  K), which also is reported in a similar system  $LaCoO_3$  [20], and with increasing temperature its electrical

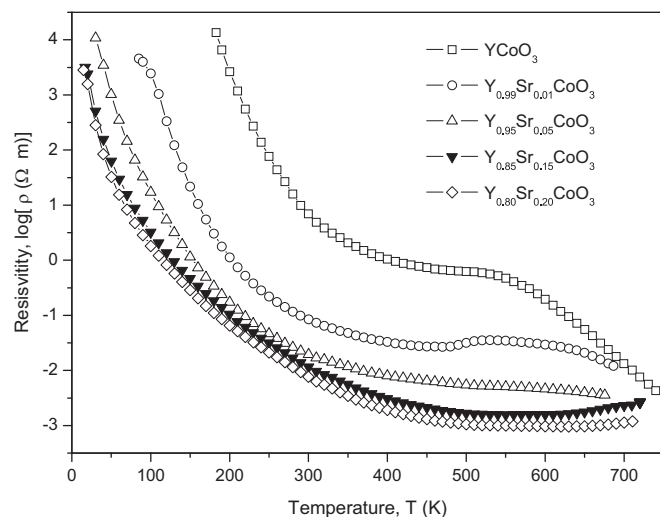


Fig. 2. Electrical resistivity  $\rho$  as a function of temperature  $T$  for  $Y_{1-x}Sr_xCoO_3$  ( $x=0, 0.01, 0.05, 0.15, 0.2$ ).

resistivity rapidly decreases to  $1.05 \Omega m$  (at 400 K); in the temperature range  $400 K < T < 550 K$  the resistivity slowly decreases to  $0.47 \Omega m$  (at 550 K), where a semiconducting state is suggested [21]; then the resistivity, again, decreases fleetingly (such as from  $0.47 \Omega m$  at 550 K down to  $7.57 \times 10^{-2} \Omega m$  at 720 K) in temperature range  $T > \sim 550 K$ , which is a transition to the higher-temperature metallic state [21]. The data of  $YCoO_3$  is basically in agreement with what is reported by Hejtmánek et al. [9,10]. After Sr substitution the electrical resistivity of  $Y_{1-x}Sr_xCoO_3$  at the same temperature decreases rapidly with increasing Sr substitution content. For example, the electrical resistivity of  $Y_{1-x}Sr_xCoO_3$  at 300 K decreases from  $6.92 \Omega m$  for  $x=0$  to  $8.45 \times 10^{-2} \Omega m$  for  $x=0.01$ , then it decreases from  $1.94 \times 10^{-2} \Omega m$  for  $x=0.05$  to  $1.15 \times 10^{-2} \Omega m$  for  $x=0.15$  and finally arrives at  $7.63 \times 10^{-3} \Omega m$  for  $x=0.2$ . The decrease in electrical resistivity may come from the decrease of distortion degree after Sr substitution (as showed by the increase of  $t$  values). The decrease of distortion with increasing Sr content will lead the average Co ( $3d$ )–O( $2p$ )–Co( $3d$ ) bond angle to tend to move toward  $180^\circ$ , making the Co( $3d$ )–O( $2p$ ) orbit overlap to become larger and interactions to become stronger. Further, this decreases the electrical resistivity of  $Y_{1-x}Sr_xCoO_3$  as the Sr content of doping increases. This explanation is consistent with what Zaanen et al. [22,23] advocated and the theoretical model [24,25].

In order to more detailedly understand the temperature behavior of electrical resistivity for  $Y_{1-x}Sr_xCoO_3$ , plots of logarithm of dc electrical resistivity  $\rho$  against reciprocal of temperature  $10^3/T$  for the compounds  $Y_{1-x}Sr_xCoO_3$  are shown in Fig. 3. We note that there are good linear relations between  $\ln \rho$  and  $1/T$  for the light substituted samples ( $x \leq 0.01$ ). However, for the heavy substituted samples ( $x \geq 0.05$ ) the relation between  $\ln \rho$  and  $1/T$  deviates seriously from the linear relationship, which results from the change of localization degree with increasing Sr substitution content, as suggested in our investigation for  $Y_{1-x}Ca_xCoO_3$  series [4,5]. The

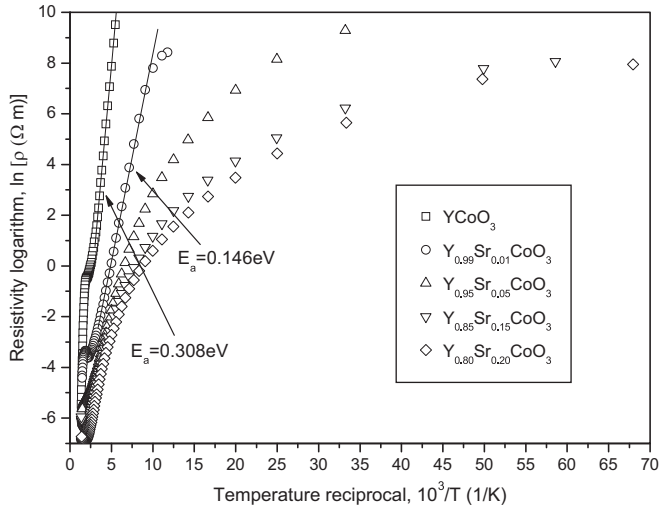


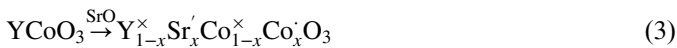
Fig. 3. Electrical resistivity logarithm  $\ln \rho$  versus temperature reciprocal  $1/T$  for  $Y_{1-x}Sr_xCoO_3$  ( $x=0, 0.01, 0.05, 0.15, 0.2$ ).

electrical resistivity data in the linear regions are fitted to Arrhenius relation

$$\rho = \rho_0 \exp\left(\frac{E_a}{k_B T}\right) \quad (2)$$

where  $\rho_0$  is a constant,  $E_a$  is the activation energy for conduction,  $k_B$ , the Boltzmann constant, and  $T$ , the absolute temperature. By best fit of the experimental data to Eq. (2) for unsubstituted sample  $x=0$  and light substituted sample  $x=0.01$ , we find out that the activation energy of conduction  $E_a$  decreases from 0.308 eV for  $x=0$  to 0.146 eV for  $x=0.01$  with increasing Sr content. This indicates from the p-type semiconductor energy band theory that the Fermi level  $E_F$  would shift toward the edge of valence band, which makes the energy difference  $E_a$  between valence band edge  $E_v$  and Fermi level to become small. This is why the electrical resistivity of  $YCoO_3$  has a large decrease after Sr substitution ( $x=0.01$ ).

From the discussion above, we know that the Sr substitution led to the decrease of electrical resistivity in  $YCoO_3$ , introducing also defects into the lattice in  $YCoO_3$ . Well then, what is the conduction carrier in  $Y_{1-x}Sr_xCoO_3$ ? The following is a qualitative discussion from the defect chemistry using the dilute solution model and the Kröger–Vink notation for  $Y_{1-x}Sr_xCoO_3$ . At high oxygen partial pressure and low temperatures the replacement of  $Y^{3+}$  by  $Sr^{2+}$  is electrically compensated by forming the  $Co^{4+}$  cation. The equation is expressed as

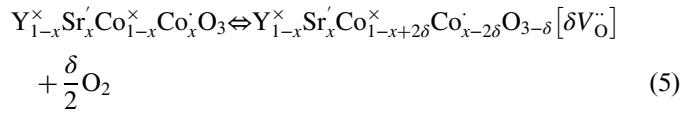


where  $Y^\times$  ( $Sr^\times$ ,  $Co^\times$  and  $Co^\cdot$ ) is a  $Y^{3+}$  ( $Sr^{2+}$ ,  $Co^{3+}$  and  $Co^{4+}$ ) cation on a  $Y^{3+}$  ( $Y^{3+}$ ,  $Co^{3+}$  and  $Co^{3+}$ ) lattice position, respectively. The electrical neutrality conduction of Eq. (3) can be written as

$$[Sr_Y^\times] = [Co_{Co}^\cdot] \quad (4)$$

At low oxygen partial pressures and/or high temperatures, the following reaction occurs with the formation of oxygen

vacancies, assuming the oxygen vacancies are doubly ionized.



The electroneutrality is the following

$$[Sr_Y^\times] = [Co_{Co}^\cdot] + 2[V_O^{\cdot\cdot}] \quad (6)$$

As suggested for  $LaCoO_3$  [26], above 200 K, its electrical conduction occurs via the transfer of electrons from low-spin cobalt ions  $Co^{III}$  ( $t_{2g}^6 e_g^0$ ) to high-spin  $Co^{3+}$  ( $t_{2g}^4 e_g^2$ ) giving rise to  $Co^{IV}$  and  $Co^{2+}$  according to the equation



This is also expected to take place in  $Y_{1-x}Sr_xCoO_3$  series. Therefore, the total expression equation is the following:

$$[Sr_Y^\times] + [Co_{Co}^\cdot] = [Co_{Co}^\cdot] + 2[V_O^{\cdot\cdot}] \quad (8)$$

That is, with increasing Sr content of substitution, the  $Co^{4+}$  increases;  $[Co_{Co}^\cdot]$  and/or  $[V_O^{\cdot\cdot}]$  can be regarded as the conduction carrier. In literature 5, we discussed that the main contribution to electrical properties of  $Y_{1-x}Ca_xCoO_3$  is  $[V_O^{\cdot\cdot}]$ -species, whereas, the contribution of  $[V_O^{\cdot\cdot}]$  species is negligibly small, indicating that the  $Co^{4+}$  exists.

### 3.3. Thermopower of $Y_{1-x}Sr_xCoO_3$

Fig. 4 presents the temperature dependence of Seebeck coefficient  $S$  for  $Y_{1-x}Sr_xCoO_3$  ( $x=0, 0.01, 0.05, 0.15, 0.20$ ) in the temperature range from 300 to 780 K. One can note that the Seebeck coefficient values for  $Y_{1-x}Sr_xCoO_3$  are all positive in the temperature range of measurement, indicating that the major carriers for conduction are holes. With increasing temperature the Seebeck coefficient of  $YCoO_3$  decreases slowly from  $\sim 1048 \mu V/K$  at 300 K to  $\sim 906 \mu V/K$  at 550 K; then it rapidly decreases to  $\sim 191 \mu V/K$  at 760 K. This behavior is in agreement with that of electrical resistivity above, and its temperature behavior here is also basically

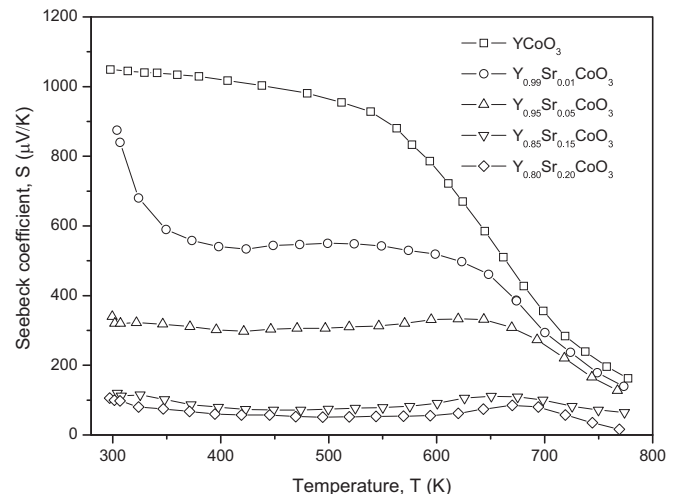


Fig. 4. Temperature dependence of Seebeck coefficient  $S$  for  $Y_{1-x}Sr_xCoO_3$  ( $x=0, 0.01, 0.05, 0.15, 0.2$ ).

consistent with those from the other authors [9,10,17]. With increasing Sr content of substitution, the temperature dependence of  $Y_{1-x}Sr_xCoO_3$  basically has no large change; however, the absolute values of Seebeck coefficient of  $Y_{1-x}Sr_xCoO_3$  decrease monotonously. For instance, at 400 K the Seebeck coefficient values decrease from 1020  $\mu V/K$  for  $x=0$  to 540  $\mu V/K$  for  $x=0.01$ , 301  $\mu V/K$  for  $x=0.05$ , 79  $\mu V/K$  for  $x=0.15$ , 59  $\mu V/K$  for  $x=0.2$ . This monotonous decrease of Seebeck coefficient for  $Y_{1-x}Sr_xCoO_3$  in the vicinity of room temperature can be estimated, based on the changes of spin states of Co ions ( $Co^{3+}$  and  $Co^{4+}$ ), by using the temperature-independent Seebeck coefficient described by so-called Heikes formula [27]

$$S = -\frac{k_B}{e} \ln \left[ \frac{g_3 y}{g_4 (1-y)} \right] \quad (9)$$

where  $g_3$  and  $g_4$  are the number of the degenerated configuration of the  $Co^{3+}$  and  $Co^{4+}$  states, respectively,  $y$  ( $=Co^{4+}/Co$ ) is the concentration of  $Co^{4+}$  holes on the Co sites. Applying this formula (9) and the Seebeck coefficient experimental values at 400 K, we obtain the  $y$  values 0.0000436, 0.0113, 0.154, 0.706, and 0.752 corresponding to the samples  $x=0$ , 0.01, 0.05, 0.15, and 0.20, respectively, assuming that the spin states of  $Co^{3+}$  and  $Co^{4+}$  at 400 K exist in low spin state  $t_{2g}^6$  and  $t_{2g}^5$ , respectively, that is,  $g_3=1$  and  $g_4=6$ . We note that the  $y$  values (concentration of  $Co^{4+}$ ) increase with increasing Sr content of substitution; this is in agreement with the above theory discussion of the Eq. (8). Therefore, the decrease of Seebeck coefficient with increasing Sr content can be well explained based on the framework of Heikes theory.

### 3.4. Power factor of $Y_{1-x}Sr_xCoO_3$

The temperature dependences of power factor  $P$  ( $=S^2/\rho$ ) for the oxides  $Y_{1-x}Sr_xCoO_3$  ( $0 \leq x \leq 0.2$ ) in the temperature range from 300 to 725 K are shown in Fig. 5. The power factor  $P$  was calculated by using the measured electrical resistivity  $\rho$

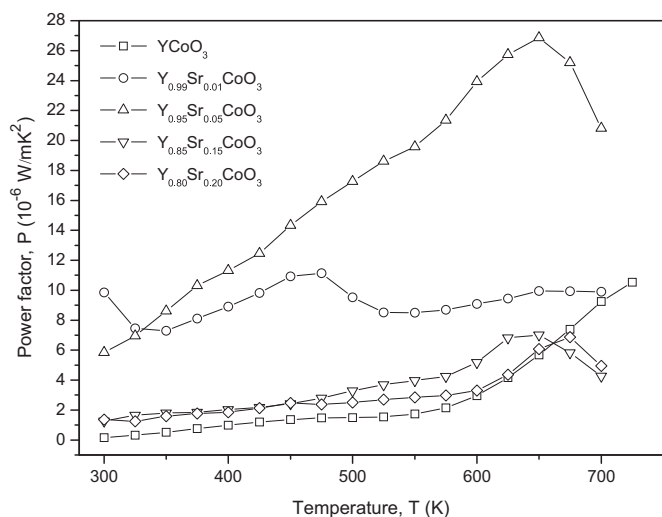


Fig. 5. Temperature dependence of power factor  $P$  for  $Y_{1-x}Sr_xCoO_3$  ( $x=0, 0.01, 0.05, 0.15, 0.2$ ).

and the Seebeck coefficient  $S$  data shown in Figs. 2 and 4, respectively. We note that  $P$  of  $Y_{1-x}Sr_xCoO_3$  increases remarkably with increasing content of Sr substitution as  $x \leq 0.5$ . For instance, at 650 K  $P$  increases from  $5.68 \times 10^{-6} W/m K^2$  for  $x=0$  to  $9.95 \times 10^{-6} W/m K^2$  for  $x=0.01$ ; then  $P$  increases to  $2.69 \times 10^{-5} W/m K^2$  as  $x$  increases to 0.05. This increase of  $P$  is mainly due to the larger decrease in the resistivity after Sr substitution. However, as  $x$  increases further to 0.2,  $P$  decreases to  $6.07 \times 10^{-6} W/m K^2$ , which mainly arises from the large decrease in Seebeck coefficient. The present result indicates that proper Sr substitution for Y in  $Y_{1-x}Sr_xCoO_3$  can effectively enhance high-temperature thermoelectric properties of  $YCoO_3$  system.

## 4. Conclusions

Strontium substituted cobalt oxides  $Y_{1-x}Sr_xCoO_3$  ( $0 \leq x \leq 0.2$ ) have been prepared by using sol-gel process and its electrical transport and thermoelectric properties have been investigated in the temperature range from 20 to 780 K. The results show that with increasing Sr content of substitution dc electrical resistivity of  $Y_{1-x}Sr_xCoO_3$  decreases remarkably, which can come from the contribution of the reduction in lattice distortion. The Seebeck coefficients of  $Y_{1-x}Sr_xCoO_3$  are all positive indicating predominant hole-type charge carriers, and they decrease monotonously with increasing Sr content of substitution, which also is explained by the Heikes equation. Moreover, experiments show that the power factor changes non-monotonously with Sr substitution with a maximum value of  $2.69 \times 10^{-5} W/m K^2$  at 650 K for the sample with  $x=0.05$ , which is about five times greater than that for  $x=0$ , indicating that appropriate Sr substitution cause effective enhancement in high-temperature thermoelectric properties of  $Y_{1-x}Sr_xCoO_3$ .

## Acknowledgments

This work was financially supported by the Key Lab of Novel Thin Film Solar Cells, Chinese Academy of Sciences (Grant no. KF201101), the Provincial Science Key Foundation of Higher Education Institutions of Anhui, China (Grant no. KJ2011A053), the Provincial Science Foundation of Higher Education Institutions of Anhui, China (Grant no. KJ2012Z034), and the National Natural Science Foundation of China (Grant nos. 51202005, 11204005, and 41075027).

## References

- [1] Edward E. Abbott, Joseph W. Kolis, Nathan D. Lowhorn, William Sams, Apparao Rao, Terry M. Tritt, Thermoelectric properties of doped titanium disulfides, *Applied Physics Letters* 88 (2006) 262106.
- [2] I Terasaki, Y. Sasago, K. Uchinokuro, Large thermoelectric power in  $NaCo_2O_4$  single crystals, *Physical Review B* 56 (1997) R12685–R12687.
- [3] J. Androulakis, J. Pantelis Migiakis, Giapintzakis,  $La_{0.95}Sr_{0.05}CoO_3$ : an efficient room-temperature thermoelectric oxide, *Applied Physics Letters* 84 (2004) 1099.
- [4] Y. Liu, X.Y. Qin, Temperature dependence of electrical resistivity for Ca-doped perovskite-type  $Y_{1-x}Ca_xCoO_3$  prepared by sol-gel process, *Journal of Physics and Chemistry of Solids* 67 (2006) 1893–1898.

- [5] Y. Liu, X.Y. Qin, Y.F. Wang, H.X. Xin, J. Zhang, H.J. Li, Electrical transport and thermoelectric properties of  $Y_{1-x}Ca_xCoO_3$  ( $0 \leq x \leq 0.1$ ) at high temperatures, *Journal of Applied Physics* 101 (2007) 083709.
- [6] Yi Liu, Haijin Li, Qing Zhang, Houtong Liu, Fabrication and thermoelectric properties of perovskite-type thermoelectric oxide  $Y_{0.95}R_{0.05}CoO_3$  ( $R=Ca, Sr, Ba$ ), *Chinese Journal of Materials Research* 26 (2012) 31–36.
- [7] Yi Liu, Qing Zhang, Haijin Li, Yong Li, Houtong Liu, Temperature dependence of electrical resistivity for Sr-doped perovskite-type oxide  $Y_{1-x}Sr_xCoO_3$  prepared by sol-gel process, *Acta Physica Sinica* 62 (2013) 047202.
- [8] Yi Liu, Haijin Li, Qing Zhang, Yong Li, Houtong Liu, Electrical transport and thermoelectric properties of Ni doped perovskite-type  $YCo_{1-x}Ni_xO_3$  ( $0 \leq x \leq 0.07$ ) prepared by sol-gel process, *Chinese Physics B* 22 (2013) 057201, <http://dx.doi.org/10.1088/1674-1056/22/5/057201>.
- [9] J. Hejtmanek, K. Knížek, H. Fujishiro, Proceedings of the 2nd European Conference on Thermoelectrics (8th European Workshop on Thermoelectrics) of European Thermoelectric Society Poland, Kraków no. 24, 2004.
- [10] J. Hejtmanek, Z. Jirák, K. Knížek, M. Maryško, M. Veverka, H. Fujishiro, Magnetism, structure and transport of  $Y_{1-x}Ca_xCoO_3$  and  $La_{1-x}Ba_xCoO_3$ , *Journal of Magnetism and Magnetic Materials* 272 (2004) E283–E284.
- [11] Apurva Mehta, R. Berliner, Robert W. Smith, The structure of Yttrium cobaltate from neutron diffraction, *Journal of Solid State Chemistry* 130 (1997) 192–198.
- [12] K. Knížek, Z. Jirák, J. Hejtmanek, M. Veverka, M. Maryško, B.C. Hauback, H. Fjellvåg, Structure and physical properties of  $YCoO_3$  at temperatures up to 1000 K, *Physical Review B* 73 (2006) 214443.
- [13] Ji-Woong Moon, Won-Seon Seo, Hiroki Okabe, Takasi Okawa, Kunihito Koumoto, Ca-doped  $RCoO_3$  ( $R=Gd, Sm, Nd, Pr$ ) as thermoelectric materials, *Journal of Materials Chemistry* 10 (2000) 2007–2009.
- [14] Ji-Woong Moon, Yoshitake Masuda, Won-Seon Seo, Kunihito Koumoto, Ca-doped  $HoCoO_3$  as p-type oxide thermoelectric material, *Materials Letters* 48 (2001) 225–229.
- [15] Ji-Woong Moon, Yoshitake Masuda, Won-Seon Seo, Kunihito Koumoto, Influence of ionic size of rare-earth site on the thermoelectric properties of  $RCoO_3$ -type perovskite cobalt oxides, *Materials Science and Engineering B* 85 (2005) 70.
- [16] C.R. Michel, A.S. Gago, H. Guzmán-Colín, E.R. López-Mena, D. Lardizábal, O.S. Buassi-Monroy, Electrical properties of the perovskite  $Y_{0.9}Sr_{0.1}CoO_{3-\delta}$  prepared by a solution method, *Materials Research Bulletin* 39 (2004) 2295–2302.
- [17] K. Knížek, Z. Jirák, J. Hejtmanek, M. Veverka, M. Maryško, G. Maris T.T.M. Palstra, Structural anomalies associated with the electronic and spin transitions in  $LnCoO_3$ , *The European Physical Journal B* 47 (2005) 213–220.
- [18] G. Demazeau, M. Pouchard, P. Hagenmuller, Sur de nouveaux composés oxygènes du cobalt +III dérivés de la perovskite, *Journal of Solid State Chemistry* 9 (1974) 202–209.
- [19] G.H. Zheng, Y.P. Sun, X.B. Zhu, W.H. Song, Structure, magnetic, and transport properties of the Co-doped manganites  $La_{0.9}Te_{0.1}Mn_{1-x}Co_xO_3$  ( $0 \leq x \leq 0.25$ ), *Solid State Communications* 137 (2006) 326–331.
- [20] K. Berggold, M. Kriener, C. Zobel, A. Reichl, M. Reuther, R. Müller, A. Freimuth, T. Lorenz, Thermal conductivity, thermopower, and figure of merit of  $La_{1-x}Sr_xCoO_3$ , *Physical Review B* 72 (2005) 155116.
- [21] G. Thornton, F.C. Morrison, S. Partington, B.C. Tofield, D.E. Williams, The rare earth cobaltates: localized or collective electron behaviour?, *Journal of Physics C: Solid State Physics* 21 (1988) 2871–2880.
- [22] J. Zaanen, G.A. Sawatzky, J.W. Allen, Band gaps and electronic structure of transition-metal compounds, *Physical Review Letters* 55 (1995) 418–421.
- [23] J. Zaanen, G.A. Sawatzky, J.W. Allen, Systematics in band gaps and optical spectra of 3D transition metal compounds, *Journal of Solid State Chemistry* 88 (1980) 8–27.
- [24] G.Ch. Kostogloudis, N. Vasilakos, Ch. Ftikos, Crystal structure, thermal and electrical properties of  $Pr_{1-x}Sr_xCoO_{3-\delta}$  ( $x=0, 0.15, 0.3, 0.4, 0.5$ ) perovskite oxides, *Solid State Ionics* 106 (1998) 207–218.
- [25] J.B. Torrance, P. Lacorre, A.I. Nazzari, E.J. Ansaldo, Ch. Niedermayer, Systematic study of insulator–metal transitions in perovskites  $RNiO_3$  ( $R=Pr, Nd, Sm, Eu$ ) due to closing of charge-transfer gap, *Physical Review B* 45 (1992) 8209–8212.
- [26] Om. Parkash, H.S. Tewari, V.B. Tare, D. Kumar, Electrical conduction in calcium yttrium titanium cobalt oxide  $Ca_{1-x}Y_xTi_{1-x}Co_xO_3$  ( $x < \text{or} = 0.15$ ), *Journal of Physics D: Applied Physics* 26 (1993) 676–679.
- [27] W. Koshibae, K. Tsutsui, S. Maekawa, Thermopower in cobalt oxides, *Physical Review B* 62 (2000) 6869–6872.